INTERNATIONAL JOURNAL FOR NUMERICAL METHODS IN ENGINEERING
Int. J. Numer. Meth. Engng 2002; **53**:1853–1869 (DOI: 10.1002/nme.365)

An implicit BEM formulation for gradient plasticity and localization phenomena

Ahmed Benallal[1,*,†], Carlos A. Fudoli[2] and Wilson S. Venturini[2]

[1] *Laboratoire de Mécanique et Technologie, ENS de Cachan/CNRS/Université Paris 6, 61 Avenue du Président Wilson, 94235 Cachan, France*
[2] *Department of Structural Engineering, São Carlos School of Engineering, University of São Paulo, Avenide Trabalhador São Corlense, 400, São Carlos, Brazil*

SUMMARY

The aim of this paper is to discuss a boundary element formulation for non-linear structural problems involving localization phenomena. In order to overcome the well-known mesh dependency observed in local plasticity, a gradient plasticity model is used. An implicit boundary element formulation is proposed and the underlying consistent tangent operator defined. This formulation is based on the classical displacement and strain integral representations combined with an integral representation of the plastic multiplier. First numerical examples are presented to illustrate the application of the method.

KEY WORDS: boundary element; localization; gradient plasticity

1. INTRODUCTION

The main objective of this paper is the application of the boundary element method (BEM) to non-linear structural problems where localization phenomena take place. Though localization phenomena were and are still extensively analysed in the context of the finite element method (FEM) [1–4] in an attempt to improve the numerical simulation of structural failures, there has been only limited interest in the context of BEM [5].

The BEM is, however, a well-established technique to deal with a large number of practical applications in engineering. In particular, the use of BEM to analyse non-linear problems has deserved special attention in the last decade. Fracture Mechanics, just to mention one example, is a very suitable kind of problem to apply the BEM techniques, because only

*Correspondence to: Ahmed Benallal, Laboratoire de Mécanique et Technologie, ENS de Cachan, 61 Avenue du Président Wilson, F-94235 Cachan Cedex, France
†E-mail: ahmed.benallal@lmt.ens-cachan.fr

Published online 27 December 2001

Received 30 December 2000
Revised 15 June 2001

the crack lines have to be discretized, saving computer time and also increasing the accuracy of the results and the confidence in the global solution [6, 7]. Problems defined over domains extending to infinity define another class where the technique is a powerful alternative to finite elements. Non-linear phenomena, such as plasticity or visco-plasticity, can also be appropriately tackled by the technique [8]. Especially for the cases that exhibit stress or strain concentration, boundary elements can be recommended. In general, the technique is able to represent well high gradients. Strain localization falls in this last class of problems which exhibit small areas of interest inside the body, where the dissipation of energy occurs, as well as rather large displacement gradients, for which the method is expected to be efficient.

The presence of strain softening (and/or non-associativity) in the constitutive behaviour brings great difficulties to classical (local) continuum theories in the description of localization phenomena. The associated boundary value-problem is no longer mathematically well-posed (see Reference [9]) after the onset of localization and local continua allow for an infinitely small bandwidth in shear or in front of a crack tip. At the numerical level, these difficulties translate into the well-known mesh dependence of solutions. Different approaches have been proposed to overcome these difficulties. One idea is to enrich the continuum with non-conventional constitutive relations in such a way that an internal or characteristic length scale is introduced. Examples of such theories are the Cosserat continua [10, 11], the gradient theories [12, 13] and the non-local models [14].

Most of the BEM techniques applied to inelastic problems are based on the integral representations of both displacements and stresses (or strains) as they follow from either the initial strain (or initial stress) method. Non-linear phenomena, such as plasticity and visco-plasticity, were treated by BEM in the early 1980s [15, 16] after the correct calculation of the free term for the initial strain tensor made by Bui [17]. Although giving good results, the BEM non-linear approaches, appearing before this decade, were all based on the very simple explicit scheme accomplished by constant matrix procedures. Implicit approaches have been proposed more recently. Jim *et al.* [18] have used implicit integration for BEM finite deformation plasticity. Telles and Carrer [19] have also proposed an implicit model to solve elasto-plastic problems in the context of dynamic analysis, for which they followed the mass matrix approach. The consistent tangent operator (CTO) has been recently introduced into the boundary element formulation by Bonnet and Mukherjee [20] and Poon *et al.* [21], using a scheme similar to the one proposed by Simo and Taylor [22] for finite elements.

In this paper, a gradient plasticity model is adopted together with the BEM for the numerical simulation of localization phenomena. The differential equation that governs the plastic multiplier is transformed to an integral representation, which together with displacement and strain integral representations will define the non-linear algebraic system of equations. This non-linear system together with the constitutive equations is solved using an implicit boundary element procedure with the consistent tangent operator. The whole procedure is started with an elastic try and then inelastic corrections follow in order to satisfy both the constitutive equations and equilibrium. All the developments to come are made for a simple isotropic hardening (softening) model. However, the procedures can be extended easily to more complex constitutive behaviour. Simple examples are then solved to demonstrate the accuracy of the technique and its capability to deal with problems where regularization of the plastic region is required.

2. CONSTITUTIVE AND FIELD EQUATIONS FOR GRADIENT PLASTICITY

2.1. Constitutive equations

The small strain gradient plasticity model taken for this work is a simple modification of the flow theory of plasticity [23–25, 12]. Let us first recall the main lines of the flow theory of plasticity with isotropic hardening.

The Cauchy stress tensor is given by

$$\boldsymbol{\sigma} = \mathbf{E} : (\boldsymbol{\varepsilon} - \boldsymbol{\varepsilon}^{\mathrm{p}}) \tag{1}$$

where $\boldsymbol{\varepsilon}$ is the total strain, $\boldsymbol{\varepsilon}^{\mathrm{p}}$ stands for the plastic strain and $\mathbf{E}$ is the matrix of elastic moduli. The yield criterion has the form

$$f(\boldsymbol{\sigma}, R(p)) \tag{2}$$

where R is the size of the yield surface and p the cumulated plastic strain defined by

$$\dot{p} = \sqrt{\tfrac{2}{3}\dot{\boldsymbol{\varepsilon}}^{\mathrm{p}} : \dot{\boldsymbol{\varepsilon}}^{\mathrm{p}}} \tag{3}$$

Plastic flow is given by the normality rule to the plastic potential F, i.e.

$$\dot{\boldsymbol{\varepsilon}}^{\mathrm{p}} = \dot{\lambda} \frac{\partial F}{\partial \boldsymbol{\sigma}} \tag{4}$$

with λ being the plastic multiplier.The plastic multiplier in Equation (4) satisfies the Kuhn–Tucker conditions, i.e.

$$\dot{\lambda} \geqslant 0, \quad f \leqslant 0, \quad \dot{\lambda} f = 0 \tag{5}$$

When it is positive, it is obtained by the consistency condition:

$$\dot{f} = 0 \tag{6}$$

Using relations (1)–(5), one can easily find

$$\dot{\lambda} = \frac{\partial f / \partial \boldsymbol{\sigma} : \mathbf{E} : \dot{\boldsymbol{\varepsilon}}}{h + \partial f / \partial \boldsymbol{\sigma} : \mathbf{E} : \partial F / \partial \boldsymbol{\sigma}} \tag{7}$$

where we have defined the plastic modulus h by

$$h = -\frac{\partial f}{\partial R} \frac{\partial R}{\partial p} \frac{\partial F}{\partial R} \tag{8}$$

Now, the simplest small strain gradient plasticity is obtained just by modifying the yield condition (2), to make the size dependent on p but also on its successive gradients. For the sake of simplicity, we consider here that f depends only on p and its Laplacian $\nabla^2 p$ and

therefore the yield criterion (2) becomes

$$f(\boldsymbol{\sigma}, R(p, \nabla^2 p)) \tag{9}$$

In this case, an explicit form for $\dot{\lambda}$ similar to Equation (7) cannot be derived.

2.2. *Field equations*

From the consistency condition (6) one can see that the plastic multiplier is governed by the following partial differential equation (see Reference [25])

$$\frac{\partial f}{\partial \boldsymbol{\sigma}} : \mathbf{E} : \dot{\boldsymbol{\varepsilon}} - H\dot{\lambda} + \omega \nabla^2 \dot{\lambda} = 0 \tag{10}$$

In this equation, we have defined

$$H = h + \frac{\partial f}{\partial \boldsymbol{\sigma}} : \mathbf{E} : \frac{\partial f}{\partial \boldsymbol{\sigma}} \tag{11}$$

$$\omega = -\frac{\partial f}{\partial R} \frac{\partial R}{\partial \nabla^2 p} \frac{\partial F}{\partial R} \tag{12}$$

From Equation (10), one can realize that the dimension of ω is H times squared length, which gives $\omega = \alpha l^2$, l being a characteristic length and α a material parameter. As the plastic multiplier is governed by a partial differential equation, one important point to discuss concerns the boundary conditions to be assumed to solve a gradient plasticity problem (see e.g. Reference [12]). There are clearly two types of boundaries to consider: the region where the plastic zone reaches the actual boundary of the body and the elastic–plastic interface. For the first case, we assume that the outward normal flux is zero,

$$\frac{\partial \dot{\lambda}}{\partial \mathbf{n}} = \mathbf{0} \tag{13}$$

while in the second case, the plastic multiplier values are zero

$$\dot{\lambda} = 0 \tag{14}$$

In this work and for sake of simplicity, we will only consider the following simple yield criterion

$$f = J_2(\sigma) - hp + \omega \nabla^2 p - \sigma_y \leqslant 0 \tag{15}$$

where h is the constant plastic modulus under homogeneous straining, σ_y the initial yield stress and ω a constant material parameter. The classical local plasticity model is recovered in the limit $\omega \to 0$. The full boundary value problem for gradient plasticity is given, therefore, by the above partial differential equation for the plastic multiplier combined with the classical equilibrium equations:

$$\operatorname{div} \boldsymbol{\sigma} + \mathbf{f} = 0 \tag{16}$$

and the appropriate boundary conditions.

3. INTEGRAL REPRESENTATION FOR INELASTIC STRUCTURES

3.1. *Integral representations of displacements, strains and stresses*

Let us first consider an isotropic elastic body. The displacement field $\mathbf{u}$ (with components u_i) satisfies the Navier's equations, i.e.

$$(-L_{ij}u_j) = -E_{ijkl}u_{k,lj} = -Gu_{i,ll} - \frac{G}{1-2\nu}u_{l,li} = b_i \tag{17}$$

where G is the shear modulus and ν Poisson's ratio.

For a domain Ω with boundary Γ, standard integral representations are derived by applying Betti's principle (or the Green's second identity). In particular, displacement, strain and stress integral representations are easily derived and may be found elsewhere (see e.g. Reference [26]),

$$c_{ik}u_k(\mathbf{x}) = -\int_\Gamma p^*_{ik}(\mathbf{x},\mathbf{Q})u_k(\mathbf{Q})\mathrm{d}\mathbf{Q} + \int_\Gamma u^*_{ik}(\mathbf{x},\mathbf{Q})p_k(\mathbf{Q})\mathrm{d}\mathbf{Q} + \int_\Omega u^*_{ik}(\mathbf{x},\mathbf{q})b_k(\mathbf{q})\mathrm{d}\mathbf{q} \tag{18}$$

$$\beta\varepsilon_{ij}(\mathbf{x}) = -\int_\Gamma p^*_{ijk}(\mathbf{x},\mathbf{Q})u_k(\mathbf{Q})\mathrm{d}\mathbf{Q} + \int_\Gamma u^*_{ijk}(\mathbf{x},\mathbf{Q})p_k(\mathbf{Q})\mathrm{d}\mathbf{Q} + \int_\Omega u^*_{ijk}(\mathbf{x},\mathbf{q})b_k(\mathbf{q})\mathrm{d}\mathbf{q} \tag{19}$$

$$\beta\sigma_{ij}(\mathbf{x}) = -\int_\Gamma S^*_{ijk}(\mathbf{x},\mathbf{Q})u_k(\mathbf{Q})\mathrm{d}\mathbf{Q} + \int_\Gamma D^*_{ijk}(\mathbf{x},\mathbf{Q})p_k(\mathbf{Q})\mathrm{d}\mathbf{Q} + \int_\Omega D^*_{ijk}(\mathbf{x},\mathbf{q})b_k(\mathbf{q})\mathrm{d}\mathbf{q} \tag{20}$$

where p_k and b_k are the traction and body force components, respectively; the symbol '*' is related to the fundamental solution corresponding to a Dirac delta distribution load applied at the collocation point $\mathbf{x}$; the free terms c_{ik} and β are dependent upon the boundary geometry (the strain and stress equation free term β is equal to $\frac{1}{2}$ for smooth points on the boundary; for non-smooth points more complex closed forms can be achieved, also including free terms in displacements); u^*_{ijk} and p^*_{ijk} are the kernels derived from Equation (18) after differentiation, while S^*_{ijk} and D^*_{ijk} are obtained after applying Hooke's law to (19).

For non-linear problems, Betti's principle cannot be directly applied. Moreover, in plasticity, the state variables are history dependent. In this case, after splitting the total strain tensor into its elastic and plastic components, the Navier's operator applies only to the elastic part, therefore Equation (17) becomes

$$(-L_{ij}u_j) = b_i - E_{ijkl}\varepsilon^{\mathrm{p}}_{kl,j} \tag{21}$$

The Somigliana's identity (18), for plasticity based on the initial stress approach, becomes

$$\begin{aligned} c_{ik}u_k(\mathbf{x}) = &-\int_\Gamma p^*_{ik}(\mathbf{x},\mathbf{Q})u_k(\mathbf{Q})\mathrm{d}\mathbf{Q} + \int_\Gamma u^*_{ik}(\mathbf{x},\mathbf{Q})p_k(\mathbf{Q})\mathrm{d}\mathbf{Q} \\ &+ \int_\Omega u^*_{ik}(\mathbf{x},\mathbf{q})b_k(\mathbf{q})\mathrm{d}\mathbf{q} + \int_\Omega \varepsilon^*_{ijk}(\mathbf{x},\mathbf{q})E_{jkrs}\varepsilon^{\mathrm{p}}_{rs}(\mathbf{q})\mathrm{d}\mathbf{q} \end{aligned} \tag{22}$$

In this equation, $\varepsilon^*_{ijk}(\mathbf{x},\mathbf{q})$ is the fundamental solution for the strains, i.e. the jk strain components at $\mathbf{q}$ when the Dirac load is applied at x in the i direction. As for the elastic case, the integral representations of strains and stresses can be obtained by differentiating (22) with respect to space co-ordinates and applying Hooke's law. Thus, one obtains

$$\beta\varepsilon_{ij}(\mathbf{x}) = -\int_\Gamma p^*_{ijk}(\mathbf{x},\mathbf{Q})u_k(\mathbf{Q})\mathrm{d}\mathbf{Q} + \int_\Gamma u^*_{ijk}(\mathbf{x},\mathbf{Q})p_k(\mathbf{Q})\mathrm{d}\mathbf{Q} + \int_\Omega u^*_{ijk}(\mathbf{x},\mathbf{q})b_k(\mathbf{q})\mathrm{d}\mathbf{q} + \int_\Omega F_{ijmk}(\mathbf{x},\mathbf{q})\varepsilon^{\mathrm{p}}_{mk}(\mathbf{q})\mathrm{d}\mathbf{q} + \beta f_{ij}(\mathbf{E}:\boldsymbol{\varepsilon}^{\mathrm{p}}) \tag{23}$$

$$\beta\sigma_{ij}(\mathbf{x}) = -\int_\Gamma S^*_{ijk}(\mathbf{x},\mathbf{Q})u_k(\mathbf{Q})\mathrm{d}\mathbf{Q} + \int_\Gamma D^*_{ijk}(\mathbf{x},\mathbf{Q})p_k(\mathbf{Q})\mathrm{d}\mathbf{Q} + \int_\Omega D^*_{ijk}(\mathbf{x},\mathbf{q})b_k(\mathbf{q})\mathrm{d}\mathbf{q} + \int_\Omega C_{ijmk}(\mathbf{x},\mathbf{q})\varepsilon^{\mathrm{p}}_{mk}(\mathbf{q})\mathrm{d}\mathbf{q} + \beta g_{ij}(\mathbf{E}:\boldsymbol{\varepsilon}^{\mathrm{p}}) \tag{24}$$

where the kernel F_{ijmk} comes from the differentiation of the strong singular domain integral containing $\varepsilon^{\mathrm{p}}_{rs}$ in (22); C_{ijmk} is achieved after applying Hooke's law, $g_{ij}(\mathbf{E}:\boldsymbol{\varepsilon}^{\mathrm{p}})$ and $f_{ij}(\mathbf{E}:\boldsymbol{\varepsilon}^{\mathrm{p}})$ are free terms that appears when performing the strong singularity derivatives. These free terms, in the particular case of plane strain problems, are given, respectively, by

$$g_{ij}(\mathbf{E}:\boldsymbol{\varepsilon}^{\mathrm{p}}) = -\frac{1}{8(1-\nu)}[2\delta_{ik}\delta_{jl} + (1-4\nu)\delta_{ij}\delta_{kl}]E_{klrs}\varepsilon^{\mathrm{p}}_{rs} \tag{25}$$

$$f_{ij}(\mathbf{E}:\boldsymbol{\varepsilon}^{\mathrm{p}}) = -\frac{1}{16G(1-\nu)}[(3-4\nu)(\delta_{ik}\delta_{jl} + \delta_{ik}\delta_{jl}) - \delta_{ij}\delta_{kl}]E_{klrs}\varepsilon^{\mathrm{p}}_{rs} \tag{26}$$

3.2. Integral representation of the plastic multiplier

For the non-local model adopted in this work the consistency condition, given in the previous section, is represented by the differential equation (10). This condition holds in the plastic region Ω^{p} over which the plastic deformation takes place. Along the boundary Γ^{p} of this plastic zone, boundary conditions must be assumed. In order to treat the whole problem under consideration with BEM, it is necessary to find the equivalent integral representation of Equation (10). As usual, several alternatives in the framework of integral equation theory can be followed to find this form. We prefer maintaining the collocation method using singular fundamental solutions to derive an appropriate plastic multiplier integral representation. Within this context, two possibilities are discussed. The simplest fundamental solution that one may adopt to derive an integral representation of the plastic multiplier is given by the solution of the following particular Poisson's equation: let us denote by $\lambda^*(\mathbf{x},\mathbf{q})$ the fundamental solution associated to the operator

$$\mathscr{L}: \mathbf{v} \to \mathscr{L}[\mathbf{v}] = \nabla^2\mathbf{v} \tag{27}$$

i.e. the solution satisfying

$$\mathscr{L}[\lambda^*(\mathbf{x},\mathbf{q})] = \delta(\mathbf{q}) \tag{28}$$

where $\delta(\mathbf{q})$ is the Dirac's distribution at $\mathbf{q}$. This solution is known and is given by

$$\lambda^*(\mathbf{x},\mathbf{q}) = \begin{cases} -\dfrac{1}{2\pi} \ln \|\mathbf{x}-\mathbf{q}\| & \text{for 2D problems} \\ \dfrac{1}{4\pi} \|\mathbf{x}-\mathbf{q}\| & \text{for 3D problems} \end{cases} \tag{29}$$

Using this fundamental solution and the Green's second identity over the plastic zone Ω^p with boundary Γ^p, the plastic multiplier λ at any point is then given by

$$c\dot{\lambda}(\mathbf{x}) = -\int_\Gamma^p \frac{\partial \lambda^*}{\partial \mathbf{n}}(\mathbf{x},\mathbf{Q})\dot{\lambda}(\mathbf{Q})\mathrm{d}\mathbf{Q} + \int_\Gamma^p \lambda^*(\mathbf{x},\mathbf{Q})\frac{\partial \dot{\lambda}}{\partial \mathbf{n}}(\mathbf{x},\mathbf{Q})\mathrm{d}\mathbf{Q}$$
$$-\int_\Omega^p \frac{H}{\omega}\lambda^*(\mathbf{x},\mathbf{q})\dot{\lambda}(\mathbf{x},\mathbf{q})\mathrm{d}\mathbf{q} - \int_\Omega^p \frac{1}{\omega}\lambda^*(\mathbf{x},\mathbf{q})\frac{\partial f}{\partial \boldsymbol{\sigma}} : \mathbf{E} : \dot{\boldsymbol{\varepsilon}}\,\mathrm{d}\mathbf{q} \tag{30}$$

It is important to note that with this simple fundamental solution, one cannot eliminate the domain integral term with density $\dot{\lambda}(\mathbf{q})$ in (30). However, as both domain integrals remaining in Equation (30) have the same kernel, no extra difficulty is expected at the numerical level.

The domain integral term with density $\dot{\lambda}(\mathbf{q})$ can be eliminated if another appropriate fundamental solution is adopted. Let us denote by $\bar{\lambda}(\mathbf{x},\mathbf{q})$ the fundamental solution associated to the operator

$$\mathscr{L} : \mathbf{v} \to \mathscr{L}[\mathbf{v}] = \nabla^2\mathbf{v} - \frac{H}{\omega}\mathbf{v} \tag{31}$$

This fundamental solution satisfies

$$\mathscr{L}[\bar{\lambda}(\mathbf{x},\mathbf{q})] = \delta(\mathbf{q}) \tag{32}$$

and is given by

$$\bar{\lambda}(\mathbf{x},\mathbf{q}) = \begin{cases} -\dfrac{1}{2\sqrt{\pi}} K_0\left(\sqrt{\dfrac{H}{\omega}}\,\|\mathbf{x}-\mathbf{q}\|\right) & \text{for 2D problems} \\ \dfrac{1}{4\pi\|\mathbf{x}-\mathbf{q}\|} \exp -\sqrt{\dfrac{H}{\omega}}\,\|\mathbf{x}-\mathbf{q}\| & \text{for 3D problems} \end{cases} \tag{33}$$

where K_0 is the modified zero-order Bessel function of the second kind.

Using this fundamental solution, one obtains the following integral representation for the plastic multiplier

$$c\dot{\lambda}(\mathbf{x}) = -\int_\Gamma^p \frac{\partial \lambda^*}{\partial \mathbf{n}}(\mathbf{x},\mathbf{Q})\dot{\lambda}(\mathbf{Q})\mathrm{d}\mathbf{Q} + \int_\Gamma^p \lambda^*(\mathbf{x},\mathbf{Q})\frac{\partial \dot{\lambda}}{\partial \mathbf{n}}(\mathbf{x},\mathbf{Q})\mathrm{d}\mathbf{Q} - \int_\Omega^p \frac{1}{\omega}\lambda^*(\mathbf{x},\mathbf{q})\frac{\partial f}{\partial \boldsymbol{\sigma}} : \mathbf{E} : \dot{\boldsymbol{\varepsilon}}\,\mathrm{d}\mathbf{q} \tag{34}$$

The only remaining domain term, in Equation (34), is independent of the plastic multiplier. Although simpler, Equation (34) can only be adopted for the particular case where the parameter H/ω is constant. Thus, for a general case one has to adopt Equation (30). Equations (30)

and (34) govern the plastic multiplier field over the plastic zone only, i.e. over the region Ω_p. During the loading process and consequently for the incremental procedure to be described latter the boundary Γ_p may move. Thus, the analysis based on those equations must be carried out in the framework of moving boundary problems, in which the final position of Γ_p is also a problem unknown.

4. TIME DISCRETIZATION: FINITE STEP PROBLEM

The starting point of the numerical formulation is the incremental form of the boundary value problem in gradient plasticity. Indeed, any numerical technique requires a space discretization of the body and a subdivision of the time interval into time steps (or the loading process into load increments). Let $\Delta t = t_{n+1} - t_n$ be a typical time step in the time discretization. The finite step boundary value problem consists of searching the solution at the end t_{n+1} of the time step when it is known at the beginning t_n. To advance the solution in time, one may use a one-parameter θ implicit time marching scheme (generalized mid-point rule). In this scheme the increment of variable z over the time step is given by

$$\Delta z = z_{n+1} - z_n = \Delta t \dot{z}_{n+\theta} \tag{35}$$

where $\dot{z}_{n+\theta}$ is the rate of z evaluated at the intermediate time $t_{n+\theta} = (1-\theta)t_n + \theta t_{n+1}$. For sake of clarity, we will develop the analysis here only for the backward Euler algorithm corresponding to $\theta = 1$. With this integration scheme, the incremental form of the plastic strain over the time step reads:

$$\Delta \boldsymbol{\varepsilon}^p = \Delta\lambda \left.\frac{\partial F}{\partial \boldsymbol{\sigma}}\right|_{n+1} = \Delta\lambda \mathbf{m}_{n+1} \tag{36}$$

where $\mathbf{m}$ is the unit outward normal to the plastic potential. The integral representations (22) and (24) take, respectively, the following incremental forms:

$$c_{ik}\,\Delta u_k = -\int_\Gamma p^*_{ik}\,\Delta u_k\,\mathrm{d}\mathbf{Q} + \int_\Gamma u^*_{ik}\,\Delta p_k\,\mathrm{d}\mathbf{Q} + \int_\Omega u^*_{ik}\,\Delta b_k\,\mathrm{d}\mathbf{q} + \int_\Omega \varepsilon^*_{ijk} E_{jkrs}\,\Delta\varepsilon^p_{rs}\,\mathrm{d}\mathbf{q} \tag{37}$$

$$\beta\,\Delta\varepsilon_{ij} = -\int_\Gamma p^*_{ijk}\,\Delta u_k\,\mathrm{d}\mathbf{Q} + \int_\Gamma u^*_{ijk}\,\Delta p_k\,\mathrm{d}\mathbf{Q} + \int_\Omega u^*_{ijk}\,\Delta b_k\,\mathrm{d}\mathbf{q} + \int_\Omega F_{ijmk}\varepsilon^p_{mk}\,\mathrm{d}\mathbf{q} + \beta f_{ij}(E_{mkrs}\,\Delta\varepsilon^p_{mk}) \tag{38}$$

while the stress increment is

$$\Delta\boldsymbol{\sigma} = \mathbf{E} : [\Delta\boldsymbol{\varepsilon} - \Delta\boldsymbol{\varepsilon}^p] \tag{39}$$

Now, if we denote by $\Omega^{\mathrm{p}}_{n+1}$ the plastic zone at the end of the time increment and $\Gamma^{\mathrm{p}}_{n+1}$ its boundary, the incremental form of the plastic multiplier integral representation is

$$c\,\Delta\lambda = -\int_{\Gamma_{+1}} \frac{\partial\lambda^*}{\partial\mathbf{n}}\Delta\lambda\,\mathrm{d}\mathbf{Q} + \int_{\Gamma_{+1}} \lambda^* \frac{\partial\Delta\lambda}{\partial\mathbf{n}}\,\mathrm{d}\mathbf{Q} - \int_{\Omega_{+1}} \frac{1}{\omega}\lambda^* \left.\frac{\partial f}{\partial\boldsymbol{\sigma}}\right|_{n+1} : \mathbf{E} : \Delta\boldsymbol{\varepsilon}\,\mathrm{d}\mathbf{q} \tag{40}$$

Note that to obtain (41), the representation (34) has been used. This is valid only if H/ω is constant. When this is not so, one should use rather (30). The corresponding integral representation of the plastic multiplier, containing an extra volume integral is

$$\begin{aligned} c\,\Delta\lambda = &-\int_{\Gamma_{+1}} \frac{\partial\lambda^*}{\partial\mathbf{n}}\Delta\lambda\,\mathrm{d}\mathbf{Q} + \int_{\Gamma_{+1}} \lambda^* \frac{\partial\Delta\lambda}{\partial\mathbf{n}}\,\mathrm{d}\mathbf{Q} \\ &- \int_{\Omega_{+1}} \lambda^* \left.\left(\frac{H}{\omega}\right)\right|_{n+1} \frac{\partial\Delta\lambda}{\partial\mathbf{n}}\,\mathrm{d}\mathbf{Q} - \int_{\Omega_{+1}} \lambda^* \left.\left(\frac{1}{\omega}\frac{\partial f}{\partial\boldsymbol{\sigma}}\right)\right|_{n+1} : \mathbf{E} : \Delta\boldsymbol{\varepsilon}\,\mathrm{d}\mathbf{q} \end{aligned} \tag{41}$$

Finally, the discrete form of the Kuhn–Tucker conditions over this increment is

$$f_{n+1} = f(\boldsymbol{\sigma}_{n+1}, \lambda_{n+1}) \leqslant 0, \quad \Delta\lambda \geqslant 0, \quad f_{n+1}\,\Delta\lambda = 0 \tag{42}$$

With the adopted time marching scheme, the initial boundary value problem for gradient plasticity is reduced to the three global and coupled integral equations (37), (38) and (41), complemented by the local expression (39) for the stresses and the constraints (42). With the relevant boundary conditions this constitutes the finite step boundary value problem. This problem is a continuous (in space) non-linear problem. Its solution can be achieved only by a space discretization and an iterative process. We first describe the space discretization and move to the solution strategy.

5. SPACE DISCRETIZATION: BOUNDARY ELEMENT FORMULATION

The continuous finite step problem described above should be discretized now in space. This is carried out here by using the BEM. The boundary of the solid is discretized into a series of elements Γ_s, over which displacement and traction increments, Δu_k and Δp_k, are interpolated in terms of their values at a series of nodal points and approximation functions. Due to the presence of domain integrals in (37), (38) and (41), the domain Ω is also divided into cells over which body forces and the plastic strains are approximated and then the corresponding domain integrals computed numerically (the plastic multiplier increments have also to be approximated if Equation (30) were adopted). Writing the discretized form of Equations (37) and (38) for the selected collocation points, a system of algebraic equations is obtained in terms of the increments of nodal values (displacements, tractions and plastic multipliers). The integral equations (37) and (38) symbolically read then (see e.g. Reference [26])

$$[\mathbf{H}^u_\Gamma]\cdot\{\Delta\mathbf{u}\} - [\mathbf{G}^u_\Gamma]\cdot\{\Delta\mathbf{p}\} = [\mathbf{T}^u_\Gamma]\cdot\{\Delta\mathbf{b}\} + [\mathbf{Q}^u_\Gamma]\cdot\{\mathbf{E} : \Delta\boldsymbol{\varepsilon}^{\mathrm{p}}\} \tag{43}$$

$$\{\Delta\boldsymbol{\varepsilon}\} = -[\mathbf{H}^u_\Omega]\cdot\{\Delta\mathbf{u}\} + [\mathbf{G}^u_\Omega]\cdot\{\Delta\mathbf{p}\} + [\mathbf{T}^u_\Omega]\cdot\{\Delta\mathbf{b}\} + [\mathbf{Q}^u_\Omega]\cdot\{\mathbf{E} : \Delta\boldsymbol{\varepsilon}^{\mathrm{p}}\} \tag{44}$$

where $\{\Delta\mathbf{u}\}$ and $\{\Delta\mathbf{p}\}$ are the vectors containing the nodal values for displacement and traction increments, respectively; $\{\Delta\boldsymbol{\varepsilon}\}$ is the vector of internal strain increments; $[\mathbf{H}^u_\Gamma]$, $[\mathbf{G}^u_\Gamma]$, $[\mathbf{T}^u_\Gamma]$, $[\mathbf{Q}^u_\Gamma]$, $[\mathbf{H}^u_\Omega]$, $[\mathbf{G}^u_\Omega]$, $[\mathbf{T}^u_\Omega]$, and $[\mathbf{Q}^u_\Omega]$ are the influence matrices arising from the numerical integration over elements and cells.

Remark: In the above relation and hereafter, the indices Γ and Ω refer to boundary and internal points, respectively. The superscripts u and λ indicate discretizations of equilibrium and consistency equations, respectively.

Applying the boundary conditions, Equations (43) and (44) are recast to

$$[\mathbf{A}^u_\Gamma]\cdot\{\Delta\mathbf{X}\} = \{\Delta\mathbf{f}^{\mathbf{u}}\} + [\mathbf{Q}^u_\Gamma]\cdot\{\mathbf{E}:\Delta\boldsymbol{\varepsilon}^{\mathrm{p}}\} \tag{45}$$

$$\{\Delta\boldsymbol{\varepsilon}\} = -[\mathbf{A}^u_\Omega]\cdot\{\Delta\mathbf{X}\} + \{\Delta\mathbf{g}^{\mathbf{u}}\} + [\mathbf{Q}^u_\Omega]\cdot\{\mathbf{E}:\Delta\boldsymbol{\varepsilon}^{\mathrm{p}}\} \tag{46}$$

where now $\Delta\mathbf{X}$ collects all the boundary unknowns while $\{\Delta\mathbf{f}^{\mathbf{u}}\}$ and $\{\Delta\mathbf{g}^{\mathbf{u}}\}$ are the contributions of prescribed boundary conditions and body forces. Equations (45) and (46) can be reduced to

$$\{\Delta\mathbf{X}\} = \{\Delta\mathbf{M}\} + [\mathbf{R}^u]\cdot\{\mathbf{E}:\Delta\boldsymbol{\varepsilon}^{\mathrm{p}}\} \tag{47}$$

$$\{\Delta\boldsymbol{\varepsilon}\} = \{\Delta\mathbf{N}\} + [\mathbf{S}^u]\cdot\{\mathbf{E}:\Delta\boldsymbol{\varepsilon}^{\mathrm{p}}\} \tag{48}$$

where $\{\Delta\mathbf{M}\}$ and $\{\Delta\mathbf{N}\}$ represent the elastic solution (displacements and strains) and the other terms are the contributions of the initial strain field. The last equation is obtained by substituting $\{\Delta\mathbf{X}\}$ from (47) into (46).

In order to build the required relations to solve the gradient plasticity problem, one has to transform Equation (41) into its algebraic form. Again, boundary and domain discretizations are required; however only the plastic region, its boundary and domain, must be considered. Boundary elements have to be defined inside the body along the plastic region front. This is made at the increment level where boundary and domain matrices must be properly defined. For simplicity and without loss of generality, the integral representation of the plastic multiplier increments Equation (41), will be adopted to perform the space discretization and to achieve the final algebraic representation. The same procedure can also be followed working on the integral representation (30). In this case an extra step will be required to transfer the coefficients related to the plastic multiplier at internal points to the boundary values. Linear elements and triangular cells with linear approximations of domain values have also been adopted to transform the plastic multiplier integral, Equation (41), into the corresponding algebraic representation. Along the boundary elements, $\Delta\lambda$ and $\Delta(\partial\lambda/\partial\mathbf{n})$ are now approximated, while the value $\partial f/\partial\boldsymbol{\sigma}:\mathbf{E}:\Delta\boldsymbol{\varepsilon}$ written in terms of strains is conveniently approximated over internal cells. Selection of collocation points and nodes follows the same strategy as for displacement and strain algebraic representations. Thus, similarly to the displacement equation case, Equation (41), for the plastic multiplier increment, can also be written in a standard manner as

$$[\mathbf{H}^\lambda_\Gamma]\cdot\{\Delta\lambda^\Gamma\} - [\mathbf{G}^\lambda_\Gamma]\cdot\left\{\frac{\partial\Delta\lambda^\Gamma}{\partial\mathbf{n}}\right\} = [\mathbf{Q}^\lambda_\Gamma]\cdot(\mathbf{m}_{n+1}:\mathbf{E}:\Delta\boldsymbol{\varepsilon}) \tag{49}$$

and for internal points, we have

$$\{\Delta\lambda\} = \{\Delta\lambda^{\Omega}\} = -[\mathbf{H}_{\Omega}^{\lambda}]\cdot\{\Delta\lambda^{\Gamma}\} + [\mathbf{G}_{\Omega}^{\lambda}]\cdot\left\{\frac{\partial\Delta\lambda^{\Gamma}}{\partial\mathbf{n}}\right\} + [\mathbf{Q}_{\Omega}^{\lambda}]\cdot(\mathbf{m}_{n+1} : \mathbf{E} : \Delta\boldsymbol{\varepsilon}) \tag{50}$$

Remark: Internal points representations are not necessary if one uses (34).

Applying the boundary conditions for the plastic multiplier, Equations (49) and (50) are recast to

$$[\mathbf{A}_{\Gamma}^{\lambda}]\cdot\{\Delta\mathbf{Y}\} = \{\Delta\mathbf{f}^{\lambda}\} + [\mathbf{Q}_{\Gamma}^{\lambda}]\cdot(\mathbf{m}_{n+1} : \mathbf{E} : \Delta\boldsymbol{\varepsilon}) \tag{51}$$

$$\{\Delta\lambda\} = -[\mathbf{A}_{\Omega}^{\lambda}]\cdot\{\Delta\mathbf{Y}\} + \{\Delta\mathbf{g}^{\lambda}\} + [\mathbf{Q}_{\Gamma}^{\lambda}]\cdot(\mathbf{m}_{n+1} : \mathbf{E} : \Delta\boldsymbol{\varepsilon}) \tag{52}$$

where again $\{\Delta\mathbf{Y}\}$ collects all the boundary unknowns while $\{\Delta\mathbf{f}^{\lambda}\}$ and $\{\Delta\mathbf{g}^{\lambda}\}$ are the contributions of prescribed boundary conditions. Substituting $\{\Delta\mathbf{Y}\}$ from (51) into (52), one obtains the following equation for the plastic multiplier at internal nodes:

$$\{\Delta\lambda^{\Omega}\} = \{\Delta\mathbf{Z}\} + [\mathbf{S}^{\lambda}]\cdot(\mathbf{m}_{n+1} : \mathbf{E} : \Delta\boldsymbol{\varepsilon}) \tag{53}$$

Therefore, the numerical analysis of gradient plasticity with BEM has been reduced to the solution of the two coupled non-linear algebraic equations, (48) and (53), for the strains and the plastic multiplier. These equations are first written in the form,

$$\mathbf{G}^{u}(\Delta\boldsymbol{\varepsilon}, \Delta\lambda) = \{\Delta\boldsymbol{\varepsilon}\} - \{\Delta\mathbf{N}\} - [\mathbf{S}^{u}]\cdot\{\mathbf{E} : \Delta\boldsymbol{\varepsilon}^{p}\} = \{\mathbf{0}\} \tag{54}$$

$$\mathbf{G}^{\lambda}(\Delta\boldsymbol{\varepsilon}, \Delta\lambda) = \{\Delta\lambda\} - \{\Delta\mathbf{Z}\} - [\mathbf{S}^{\lambda}]\cdot(\mathbf{m}_{n+1} : \mathbf{E} : \Delta\boldsymbol{\varepsilon}) = \{\mathbf{0}\} \tag{55}$$

Remark: Particular attention must be paid when choosing the boundary elements and cells and also the approximation functions. In order to obtain the algebraic representations straight linear elements with linear approximations have been adopted to transform the boundary terms. The domain integrals have been performed using linear approximations over triangular cells. In order to guarantee the validity of Equations (23) and (24) with $\beta = 0.5$, strains have been computed at boundary nodes defined inside the elements (given by the dimensionless co-ordinates equal to $\xi = \pm 0.5$) (see Reference [27]).

6. SOLUTION STRATEGY

To start the numerical process, an elastic trial is made. The first iteration is then elastic and we have from (47) and (48)

$$\begin{aligned} \{\Delta\mathbf{X}^{t}\} &= \{\Delta\mathbf{M}\} \\ \{\Delta\boldsymbol{\varepsilon}^{t}\} &= \{\Delta\mathbf{N}\} \end{aligned} \tag{56}$$

The elastic stress increments are computed $\Delta\boldsymbol{\sigma} = \mathbf{E} : \Delta\boldsymbol{\varepsilon}$. Next, the yield criterion is checked. One computes then

$$f_{n+1}^{t} = J_2(\boldsymbol{\sigma}_{n+1}^{t}) - H\lambda_n + \omega\nabla^2\lambda_n \tag{57}$$

If for all internal points we have $f_{n+1}^{t} < 0$, then the behaviour is elastic and the calculation is completed. Otherwise, plastic corrections should be applied in order to satisfy the constitutive equations and to bring the stresses on the yield surface. This is done by solving iteratively the non-linear problem given by Equations (54) and (55) subjected to the constraints (42). This system is solved by a Newton–Raphson scheme. Therefore, the additive corrections $\delta\boldsymbol{\varepsilon}^i = \Delta\boldsymbol{\varepsilon}^{i+1} - \Delta\boldsymbol{\varepsilon}^i$ to $\Delta\boldsymbol{\varepsilon}^i$ and $\delta\lambda^i = \Delta\lambda^{i+1} - \Delta\lambda^i$ to $\Delta\lambda^i$ are given by

$$[\mathbf{H}^i] \cdot \begin{Bmatrix} \delta\boldsymbol{\varepsilon}^i \\ \delta\lambda^i \end{Bmatrix} = \begin{bmatrix} \dfrac{\partial \mathbf{G}}{\partial \Delta\boldsymbol{\varepsilon}} & \dfrac{\partial \mathbf{G}}{\partial \Delta\lambda} \\ \dfrac{\partial G}{\partial \Delta\boldsymbol{\varepsilon}} & \dfrac{\partial G}{\partial \Delta\lambda} \end{bmatrix} \cdot \begin{Bmatrix} \delta\boldsymbol{\varepsilon}^i \\ \delta\lambda^i \end{Bmatrix} = - \begin{Bmatrix} \mathbf{G}^u(\Delta\boldsymbol{\varepsilon}^i, \Delta\lambda^i) \\ G^\lambda(\Delta\boldsymbol{\varepsilon}^i, \Delta\lambda^i) \end{Bmatrix} = \mathbf{R}^i \tag{58}$$

where $[\mathbf{H}]$ is the global consistent tangent operator. The iterative process is stopped when the yield function f_{n+1} and the residual $\mathbf{R}^i$ are, respectively, smaller than some fixed tolerances η and η'.

Remark: To check the yield condition, one needs the Laplacian $\nabla^2\lambda$. This is not furnished by the integral representation. However, one can obtain its values by considering the incremental form of the original consistency condition (10), i.e.

$$\left.\frac{\partial f}{\partial \boldsymbol{\sigma}}\right|_{n+1} : \mathbf{E} : \Delta\boldsymbol{\varepsilon} - H\Delta\lambda + \omega\nabla^2\Delta\lambda = 0 \tag{59}$$

after getting $\Delta\lambda$ and $\Delta\boldsymbol{\varepsilon}$ by solving the global integral equations (54) and (55).

The consistent tangent operator is computed now in closed form using relations (54) and (55). From there, one obtains

$$[\mathbf{H}] = \begin{pmatrix} \mathbf{I} - [\mathbf{S}^u] \cdot \left[\Delta\lambda \mathbf{E} : \dfrac{\partial \mathbf{m}_{n+1}}{\partial \Delta\boldsymbol{\varepsilon}} \right] & -[\mathbf{S}^u] \cdot \left\{ \mathbf{E} : \mathbf{m}_{n+1} + \Delta\lambda \mathbf{E} : \dfrac{\partial \mathbf{m}_{n+1}}{\partial \Delta\lambda} \right\} \\ -[\mathbf{S}^\lambda] \cdot \left\{ \mathbf{E} : \mathbf{m}_{n+1} + \dfrac{\partial \mathbf{m}_{n+1}}{\partial \Delta\boldsymbol{\varepsilon}} : \mathbf{E} : \Delta\boldsymbol{\varepsilon} \right\} & \mathbf{I} - [\mathbf{S}^\lambda] \cdot \left[\dfrac{\partial \mathbf{m}_{n+1}}{\partial \Delta\lambda} : \mathbf{E} : \Delta\boldsymbol{\varepsilon} \right] \end{pmatrix} \tag{60}$$

After choosing the plastic potential F, one can derive the derivatives of its normal $\mathbf{m}_{n+1}$ with respect to increments of strain $\Delta\boldsymbol{\varepsilon}$ and plastic multiplier $\Delta\lambda$. In the sequel, these are given in closed forms for the particular and simpler case of non-local associative J_2 plasticity theory, i.e. when $f = F$ and f is given by (15). The following expressions are easily derived:

$$\frac{\partial \mathbf{m}_{n+1}}{\partial \Delta\boldsymbol{\varepsilon}} = \frac{2G}{J_2(\boldsymbol{\sigma}_{n+1}) + 2G\Delta\lambda} \left\{ \mathbf{I} - \frac{1}{3}\mathbf{1} \otimes \mathbf{1} - \mathbf{m}_{n+1} \otimes \mathbf{m}_{n+1} \right\} \tag{61}$$

$$\frac{\partial \mathbf{m}_{n+1}}{\partial \Delta\lambda} = \mathbf{0} \tag{62}$$

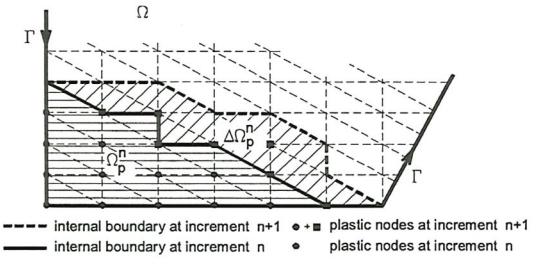

Figure 1. Internal boundary definition.

In this last expression, $\mathbf{I}$ is the fourth order tensor, $\mathbf{1}$ is the second order unit tensor while $\otimes$ denotes the tensorial product. One should notice here that just as for local J_2 plasticity, the plastic correction of the adopted algorithm corresponds to a radial return to the yield surface from the elastic trial. Indeed, this stress trial $\boldsymbol{\sigma}_{n+1}^{\mathrm{t}}$ is

$$\boldsymbol{\sigma}_{n+1}^{\mathrm{t}} = \boldsymbol{\sigma}_n + \mathbf{E} : \Delta\boldsymbol{\varepsilon} \tag{63}$$

from which we can also find the deviatoric stress trial $\mathbf{s}_{n+1}^{\mathrm{t}}$ as

$$\mathbf{s}_{n+1}^{\mathrm{t}} = \mathbf{s}_n + \mathbf{E} : \Delta\mathbf{e} \tag{64}$$

where $\Delta\mathbf{e}$ is the deviatoric part of the strain increment. The constitutive equation (39) now reads

$$\Delta\boldsymbol{\sigma} = \mathbf{E} : (\Delta\boldsymbol{\varepsilon} - \Delta\lambda\mathbf{m}_{n+1}) \tag{65}$$

From this last equation, one can compute the deviatoric stress at the end of the increment as

$$\mathbf{s}_{n+1} = \mathbf{s}_{n+1}^{\mathrm{t}} - 2G\Delta\lambda \tag{66}$$

As $\mathbf{m}_{n+1} = \mathbf{s}_{n+1}/J_2$, one concludes just as in the local case that $\mathbf{s}_{n+1}$ is colinear to $\mathbf{s}_{n+1}^{\mathrm{t}}$. The stress at the end of the increment is obtained by returning radially from the elastic trial to the yield surface.

Another important aspect of the implementation is related to the moving boundary of the plastic zone. This can be done in a rigorous way but at the price of more computational effort. Indeed at each iteration, after checking the yield condition, the active plastic zone is obtained. One can therefore define its boundary and write properly the corresponding integral representation. The iteration process when converging will lead to the actual elastic–plastic boundary. The most difficult step in doing so is the definition of the active plastic zone and the associated practical difficulties. Another rigorous strategy in the same lines as that developed by Liebe *et al.* [28] for finite elements is under investigation.

In this paper, a simpler procedure is used where the second term on the right-hand side of (40) has been neglected. The first term on the right-hand side of (40) vanishes owing to boundary conditions (14). Therefore, only the domain integral remains. One needs only to define at each iteration the plastic zone: all cells containing at least one active plastic node are included in the plastic zone. This is schematically shown in Figure 1.

The general scheme of the algorithm for solving gradient plasticity in the framework of BEM is sketched below for a load increment:

1. Initialization: $i=0, \quad (\varepsilon^{p}_{n+1})^0=\varepsilon^{p}_{n}, \quad \lambda^0_{n+1}=\lambda_n$
2. Compute trial elastic strains and stresses
3. Check yield condition at all internal node points.
   if $f(\sigma_{n+1},\lambda_{n+1},\nabla^2\lambda_n)<0$ everywhere, then EXIT
4. Otherwise define the active plastic zone Ω^{pa}_{n+1}. Compute consistent tangent operator $\mathbf{H}$ and solve (58) for incremental strains $\Delta\varepsilon^i_{n+1}$ and incremental plastic multipliers $\Delta\lambda^i_{n+1}$. Update plastic strains, stresses,...
5. Check convergence of the Newton–Raphson's process
   if $f(\sigma^i_{n+1},\lambda^i_{n+1},\nabla^2\lambda^i_{n+1})<\eta$ and $\mathbf{R}^i_{n+1}<\eta'$, then EXIT.
   Otherwise set $i=i+1$ and Go to 3

7. NUMERICAL EXAMPLE

This section is devoted to the first applications of the boundary element formulation described above for gradient plasticity and localization phenomena. First, we present some results obtained with BEM for local plasticity and the implicit formulation using the consistent tangent operator. These results show, as expected, the classical mesh dependency in presence of softening. We noted that convergence is obtained only with coarse meshes for this problem when using the explicit formulation. These results are, however not reported here. In a second stage, we show how the gradient plasticity model is able to regularize the computations.

A rectangular block is considered and is subjected to compression along its right side and the analysis is carried out under plane strain conditions. This example was extensively analysed in the literature in the context of finite elements. The gradient plasticity model presented in previous sections was used with the following constitutive parameters:

Young's modulus: $E=2000$ MPa
Poisson's ratio: $v=0.20$
Softening modulus: $h=-0.01234$, $E=-24.6$ MPa

The parameter ω was varied in the calculations and will be given when necessary. Figure 2 shows the geometry of the block and its dimensions, the loading conditions, the boundary conditions and also the coarse mesh (containing 128 cells) used in the analysis. Two other (regular) finer discretizations, containing 512 and 2048 cells, respectively, were also considered to measure the mesh dependency.

To trigger the localization phenomenon, an asymmetric weaker zone (see Plate 1) in the block was considered. The yield stress is equal to 2.0 MPa everywhere in the mesh except over the weaker zone. There, the yield stress is reduced by 0.2 MPa at the central node. For the other points, the reduction varies linearly from the centre up to the square boundary.

A uniform displacement without shear is applied to the right side of the block. Several increment sizes have also been tested to analyse how the developed procedure behaves. The results presented here were obtained with 400 load increments.

Figure 3 shows the load–displacement response for the three considered discretizations when the constitutive behaviour is modelled by classical local plasticity. The mesh dependency

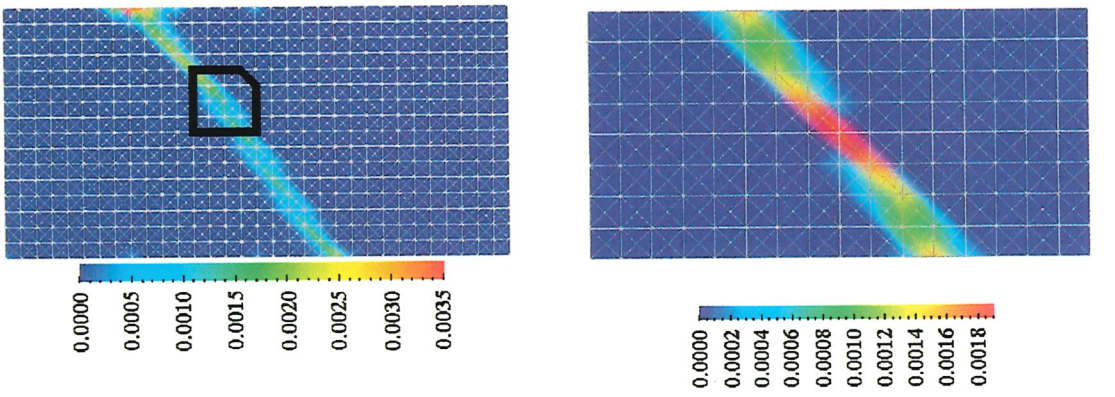

Plate 1. Distribution of equivalent plastic strain over the block for the two finest discretizations and local plasticity. The width of the localized zone is set always by the mesh size.

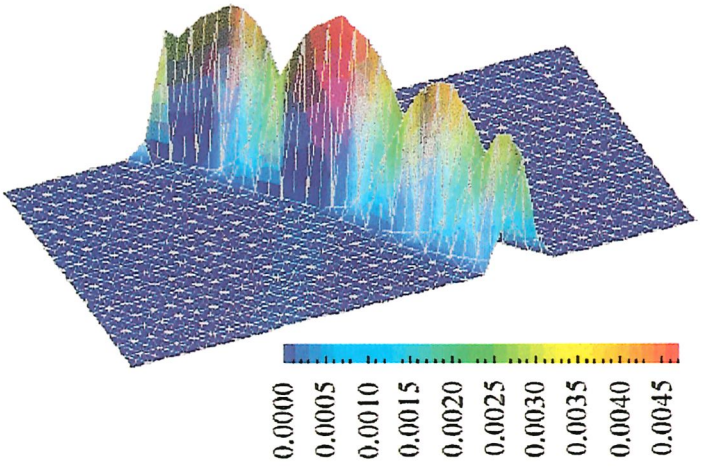

Plate 2. Three-dimensional visualization of the equivalent plastic strain field for the finest mesh and local plasticity.

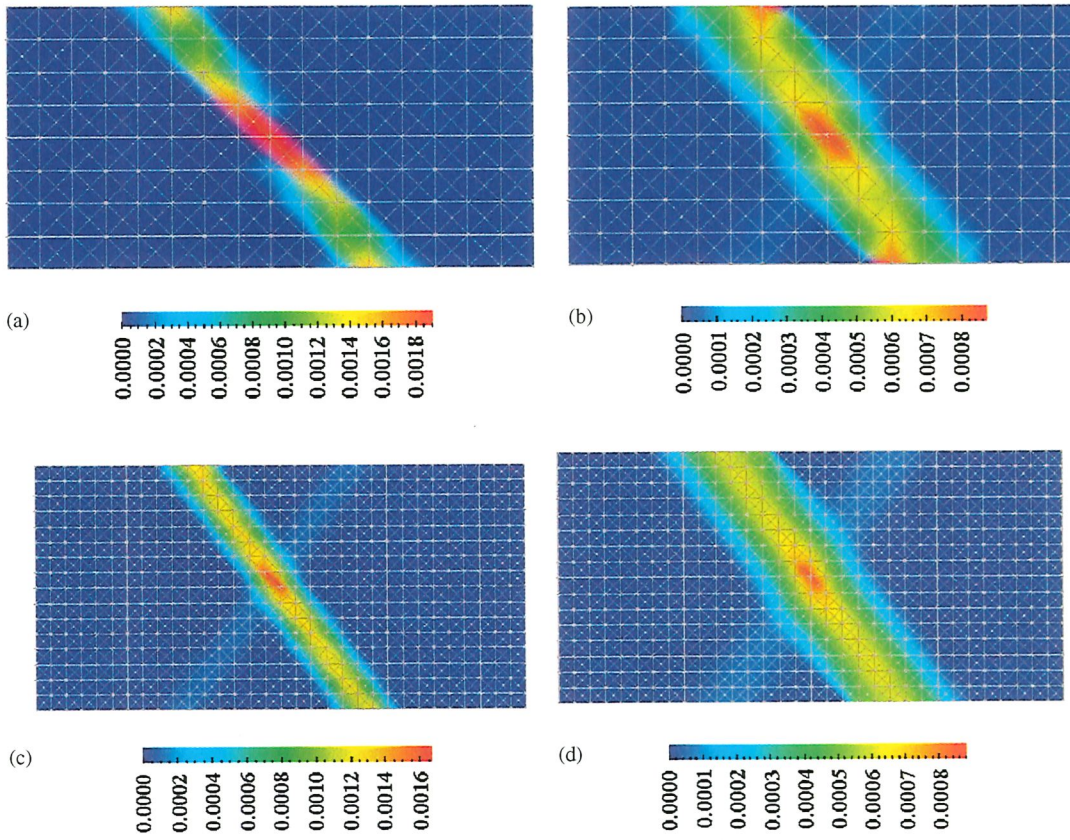

Plate 3. Distribution of equivalent plastic strain for the two finest meshes with $\omega = 1000$ (a,c) and $\omega = 5000$ (b,d).

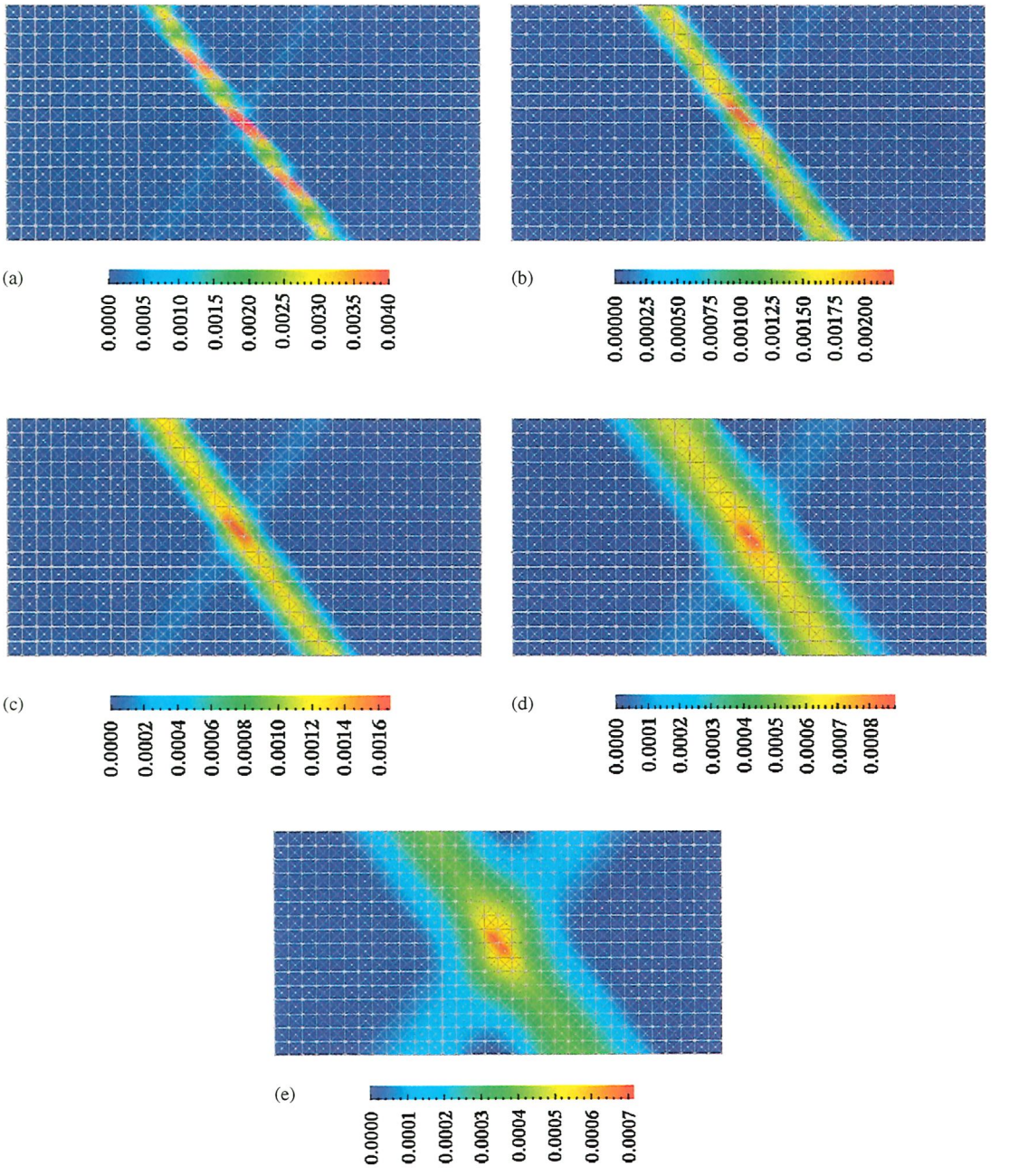

Plate 4. Distribution of equivalent plastic strain for the finest mesh with $\omega = 0.01$ (a), $\omega = 500$ (b), $\omega = 1000$ (c), $\omega = 5000$ (d), $\omega = 10\,000$ (e).

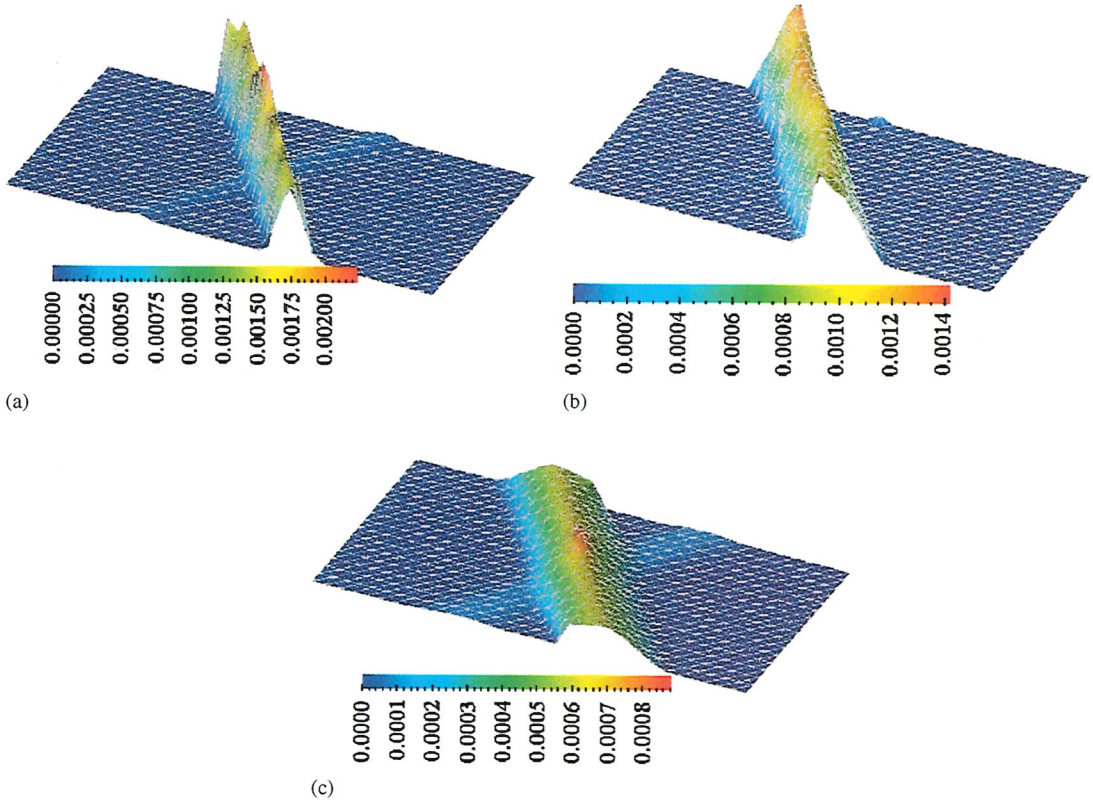

Plate 5. Three-dimensional visualization of the equivalent plastic strain field for the finest mesh and $\omega = 500$ (a), $\omega = 1000$ (b), $\omega = 5000$ (c).

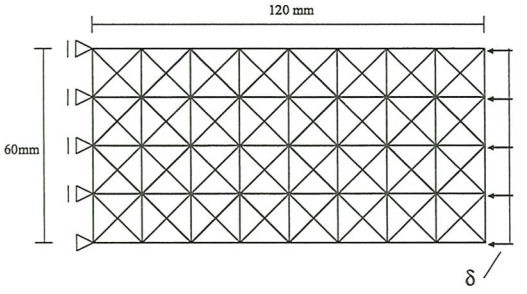

Figure 2. Rectangular block: dimensions, boundary conditions, loading and coarse discretization (128 cells); $E = 2000$ MPa, $h = -0.0125E$, $\sigma_y = 2$ MPa.

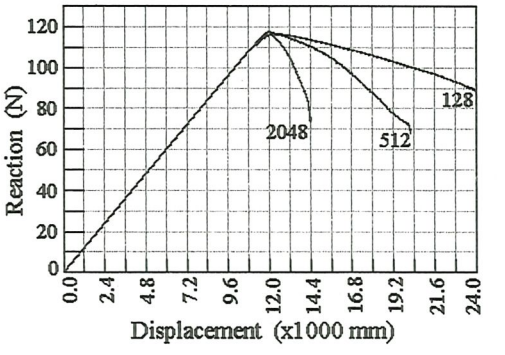

Figure 3. Load–displacement response curves for the three discretizations (128, 512 and 2048 cells) and local plasticity.

appears clearly in this figure. With the finest mesh the response is steeper after the peak showing the possibility of snap-back behaviour if further refinement was made. The smallest slope is obtained using 128 cells; as the cell size is large in this case, the dissipation zone is large too. For all analysed cases, the internal cell size defines the dissipation zone width. The results obtained by using the consistent tangent operator is far better when compared with the ones computed by the classical constant matrix BEM. Using the standard scheme, the mesh dependence was of course also detected, but the results are highly unstable in comparison with the implicit scheme.

The solution obtained by using the consistent operator is shown in Plate 1 with a clear localized diagonal narrow zone. This narrow zone is always precisely defined over about a row of cells. Thus, the width of this zone is defined by the mesh size. No plastic strain develops out of that zone. The weaker zone is also displayed. Its asymmetry guarantees that only one band will develop at least in the beginning of the deformation. Another representation (three-dimensional view) for the localization phenomenon in the case of local plasticity is shown in Plate 2.

Plate 3 illustrates the capability of the proposed BEM scheme to capture the localized zone when the material behaviour is modelled by gradient plasticity. One can see that the plastic zone is now a narrow zone but containing several rows of cells. For two different values of ω, this figure shows the localized zone for two different discretizations where the differences with local plasticity can be seen. In particular, the width of the localized zone is changing a little from one discretization to the other (at constant ω). This surely needs confirmation by further refinement of the discretization.

Figure 4 shows the load–displacement responses for the three discretizations when using the gradient plasticity model with $\omega = 500$. One can see clearly there that the three responses are almost the same showing the regularizing effect of gradient plasticity and objectivity of the computations.

Plate 4 represents the localized zone for the finest mesh and different values of the gradient plasticity model parameter ω. Five values were considered and are given in the figure. As expected, the width of the localized zone is increasing with increasing ω. The corresponding load–displacement curves are given in Figure 5 where the role of ω is clearly seen. Finally,

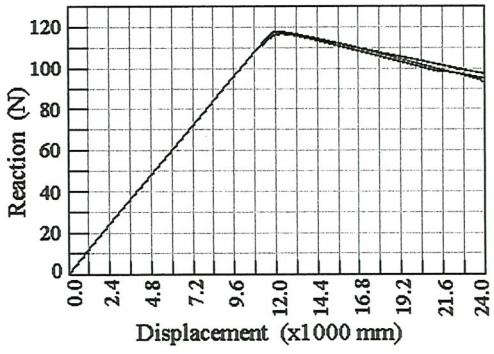

Figure 4. Load–displacement curves for the three discretizations and with gradient plasticity model with $\omega = 500$.

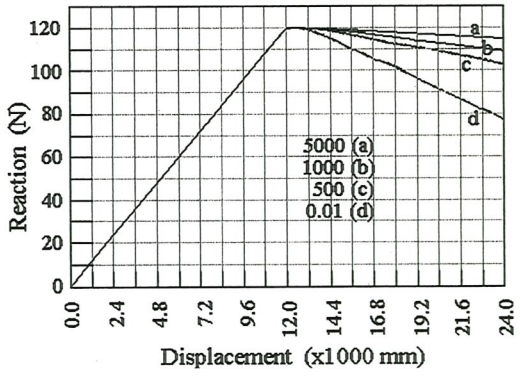

Figure 5. Load–displacement curves for the finest discretization with $\omega = 5000$ (a), $\omega = 1000$ (b), $\omega = 500$ (c), $\omega = 0.01$ (d).

three-dimensional visualizations of the deformation are also provided in Plate 5 for the same discretization and the values 500, 1000 and 5000 for ω.

8. CONCLUSIONS

The paper has demonstrated the feasibility of the boundary element method in the analysis of localization phenomena. Implicit BEM scheme has been proposed here for gradient plasticity and the underlying consistent tangent operator was defined. It appears to be a robust tool for the solution. The extension to more complex behaviour including damage for instance is under way as is the implementation of the necessary arc-length control techniques in this type of problems.

REFERENCES

1. de Borst R. Bifurcations in finite element models with a non-associated flow law. *International Journal for Numerical and Analytical Methods in Geomechanics* 1988; **12**:99–116.
2. Bazant ZP, Belytschko TB, Chang TP. Continuum theory for strain softening. *Jouranl of Engineering and Mechanical Division, ASCE* 1984; **110**:1666–1692.
3. Loret B, Prevost JH. Dynamic strain localisation in fluid-saturated porous media. *Journal of Engineering Mechanics, ASCE* 1991; **117**:907–922.
4. Schrefler BA, Majorana CO, Sanavia L. Shear band localization in saturated porous media. *Archives of Mechanics* 1995; **47**:5177–5199.
5. Maier G, Miccoli S, Novati G, Perego U. Symmetric Galerkin boundary element method in plasticity and gradient plasticity. *Computational Mechanics* 1995; **17**:115–129.
6. Aliabadi MH, Rooke DP. *Numerical Fracture Mechanics*. Computer Mechanics Publications, Kluwer Academic Publishers: Dordrecht, 1991.
7. Cruse TA. *Boundary Element Analysis in Computational Fracture Mechanics*. Kluwer Academic Publishers: Dordrecht, 1988.
8. Brebbia CA, Telles JCF, Wrobel LC. *Boundary Element Techniques. Theory and Applications in Engineering*. Springer: Berlin, 1984.
9. Benallal A, Billardon R, Geymonat R. Some mathematical aspects of the damage softening problem. In *Cracking and Damage*, Mazars J, Bazant ZP (eds), vol. 1. 1988; 247–258.
10. Mulhaus HB, Vardoulakis I. The thickness of shear bands in granular materials. *Geotechnique* 1987; **37**:271–283.

11. de Borst R. Simulation of strain localisation: A reappraisal of the cosserat continuum. *Engineering Computations* 1991; **8**:317–332.
12. de Borst R, Mulhaus HB. Gradient dependent plasticity: formulation and algorithmic aspects. *International Journal for Numerical Methods in Engineering* 1992; **35**:521–540.
13. Lasry D, Belytschlo T. Localisation limiters in transient problems. *International Journal of Solids and Structures* 1988; **24**:581–597.
14. Pijaudier-Cabot G, Bazant ZP. Nonlocal damage theory. *Journal of Engineering Mechanics, ASCE* 1987; **113**:1512–1533.
15. Telles JCF. *The Boundary Element Method Applied to Inelastic Problems.* Springer: Berlin, 1983.
16. Venturini WS. *Boundary Element Method in Geomechanics.* Springer: Berlin, 1983.
17. Bui HD. Some remarks about the formulation of three-dimensional thermoelastic problems by integral equations. *International Journal of Solids and Structures* 1978; **14**:935–939.
18. Jim H, Runesson K, Matiasson K. Boundary element formulation in finite deformation plasticity using implicit integration. *Computers and Structures* 1989; **31**:25–34.
19. Telles JCF, Carrer JAM. Static and dynamic non-linear stress analysis by the boundary element method with implicit techniques. *Engineering Analysis with Boundary Elements* 1994; **14**:65–74.
20. Bonnet M, Mukherjee S. Implicit BEM formulation for usual and sensitivity problems in elasto-plasticity using the consistent tangent operator concept. *International Journal of Solids and Structures* 1996; **33**:4461–4480.
21. Poon H, Mukherjee S, Bonnet M. Numerical implementation of a CTO-based implicit approach for the BEM solution of usual and sensitivity problems in elasto-plasticity. *Engineering Analysis with Boundary Elements* 1998; **22**:257–269.
22. Simo JC, Taylor RL. Consistent tangent operators for rate-independent elastoplasticity. *Computational Methods in Applied Mechanics and Engineering* 1985; **48**:101–118.
23. Aifantis EC. Contemporary topics in plastic deformation: Anisotropy, textures, voids and shear bands. In *Yielding, Damage and Failure of Anisotropic Solids*, Boehler IP (ed.), Proceedings of the IUTAM/ICM Symposium A. Sawczuk in Memoriam. 1987; 319–333.
24. Mulhaus HB, Aifantis E. A variational principle in gradient plasticity. *International Journal of Solids and Structures* 1991; **28**:1761–1775.
25. Benallal A, Tvergaard V. Nonlocal continuum effects on bifurcation in the plane strain tension–compression test. *Journal of Mechanics and Physics of Solids* 1995; **43**:741–770.
26. Bonnet M. *Equations Intégrales et Eléments de frontière.* CNRS Editions/Eyrolles: Paris, 1995.
27. Guiggiani M. Hypersingular formulation for boundary stress evaluation. *Engineering Analysis with Boundary Elements* 1994; **13**:169–179.
28. Liebe T, Steinmann P, Benallal A. Computational aspects of a thermodynamically consistant gradient damage. *Computational Methods in Applied Mechanics and Engineering* 2001, in press.

